CRYSTAL GROWTH & DESIGN

pubs.acs.org/crystal

Article

Refine Intervention: Characterizing Disordered $Yb_{0.5}Co_3Ge_3$

Published as part of a Crystal Growth and Design virtual special issue on The Rietveld Refinement Method: Half of a Century Anniversary

Ashley Weiland, Lucas J. Eddy, Gregory T. McCandless, Halyna Hodovanets, Johnpierre Paglione, and Julia Y Chan*

Cite This: *Cryst. Growth Des.* 2020, 20, 6715−6721

Read Online

ACCESS | Metrics & More | Article Recommendations

ABSTRACT: Single crystals of the ternary $Yb_{0.5}Co_3Ge_3$ have been grown out of molten Sn flux and characterized by single crystal and synchrotron powder X-ray diffraction. $Yb_{0.5}Co_3Ge_3$ adopts a hybrid YCo_6Ge_6/CoSn structure, crystallizing in the hexagonal space group *P6/mmm* with lattice parameters $a \approx 5.1$ Å and $c \approx 3.9$ Å. Although the compound does not magnetically order down to 2 K, Weiss temperatures of −21 K, −18.7 K, and −21 K for H//*a*, H//*c*, and the polycrystalline average, respectively, indicate antiferromagnetic interactions with $\mu_{eff} = 4.23\ \mu_B$, slightly lower than the full Yb^{3+} moment of 4.54 μ_B. Field-dependent magnetization up to 7 T measured at 2, 5, and 10 K show a linear dependence along H//*a*. Magnetization at 2 K for H//*c* approaches saturation near 1 μ_B, lower than the full Yb^{3+} moment. Herein, we present the synthesis and characterization of $Yb_{0.5}Co_3Ge_3$.

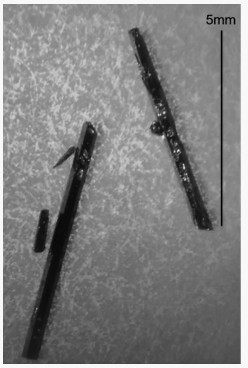

1. INTRODUCTION

While pursuing the growth of single crystals of ytterbium-based germanides following the discovery of $Ln_3Co_{2+x}Ge_{7-y}Sn_y$ (Ln = Pr, Nd, Sm)[1] and $Ce_6Co_5Ge_{16}$[2] of the new homologous series $A_{n+1}B_nX_{3n+1}$ (A = rare earth, B = transition metal, X = Ge/Sn),[3] the intermetallic compound with the formula $Yb_{0.4633(9)}Co_3Ge_3$ (denoted as $Yb_{0.5}Co_3Ge_3$ for simplicity) was grown. Although a previously reported structure,[4,5] further analysis suggests possible disorder that differs from the previous $YbCo_6Ge_6$. The newly synthesized $Yb_{0.5}Co_3Ge_3$ structure can be described as a hybrid of YCo_6Ge_6 and CoSn structure types, where the former structure type is the most dominant.

The introduction of the binary CoSn structure type (or B35), consisting of graphite-like Sn nets and Kagome nets of Co centered by Sn atoms, is of interest as the CoSn structure type provides a robust platform to study the interplay of d- and f-electrons. Additionally, the CoSn structure type provides the potential for frustration and depending on interlayer couplings, a ferromagnetic alignment of transition metal spins that can develop in the kagome layer. The kagome net, named after the knitting pattern it resembles, can be described as a group of interconnected triangles and hexagons. Kagome nets have been shown to host a giant anomalous Hall effect in Fe_3Sn_2,[6] half-metallic ferromagnetism and a zero-field Nernst effect in $Co_3Sn_2S_2$,[7−9] and a planar flat band in YCr_6Ge_6.[10] The structural stability of the kagome lattice CoSn is intriguing due to the unusual large void space.[11,12] Much attention has been focused on the large void spaces in the CoSn structure type, which can be described as an alternating layer of hexagons. The origin layer ($z = 0$) is comprised of Co edge-sharing hexagons filled with Sn1 atoms, while the *ab*-plane halfway up the *c*-axis ($z = 1/2$) is composed entirely of Sn2 edge-sharing hexagons with a large void space in the center. This void space possesses a maximal diameter of approximately 6.08 Å along the *a*−*b* plane and a 4.26 Å distance along the *c*-axis between the centers of neighboring Sn1 atoms.[13] $Yb_{0.5}Co_3Ge_3$, of the YCo_6Ge_6 type, can be described as an insertion of rare earth elements in the CoSn structure. Recently, Dirac Fermions and flat bands have both been observed in the antiferromagnetic kagome metal FeSn, which crystallizes in the CoSn structure type.[14] Herein, we report the crystal growth, structural determination by single crystal and synchrotron powder X-ray diffraction, and magnetic and electrical properties of $Yb_{0.5}Co_3Ge_3$.

2. EXPERIMENTAL SECTION

2.1. Synthesis of $Yb_{0.5}Co_3Ge_3$. Single crystals of $Yb_{0.5}Co_3Ge_3$ were grown from a molten Sn flux using the flux growth method.[15−17]

Received: June 23, 2020
Revised: August 26, 2020
Published: August 27, 2020

https://dx.doi.org/10.1021/acs.cgd.0c00865
Cryst. Growth Des. 2020, 20, 6715−6721

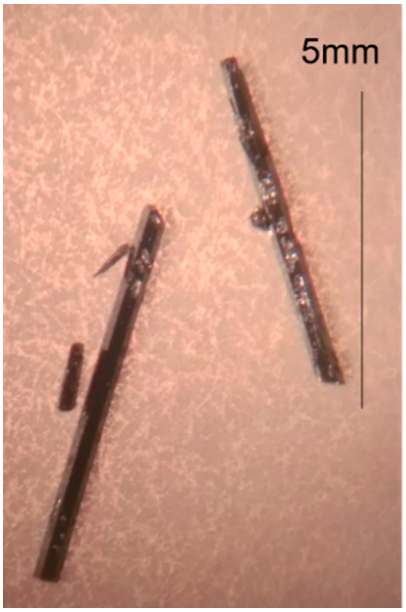

Figure 1. Crystals of $Yb_{0.5}Co_3Ge_3$ up to ~5 mm long.

Table 1. Single Crystal Data and Refinement Parameters for $Yb_{0.5}Co_3Ge_3$

space group	*P6/mmm*
a (Å)	5.0949(10)
c (Å)	3.9136(9)
V (Å^3)	87.98(4)
Z	1
temperature (K)	298
θ (deg)	4.6–38.1
μ (mm^{-1})	51.02
reflections	7685
unique reflections	144
GOF	1.34
R_1	0.014
wR_2	0.028
$\Delta\rho_{max}$ (e Å^{-3})	1.27
$\Delta\rho_{min}$ (e Å^{-3})	−1.14

Yb, Co, Ge, and Sn were combined in a 3:2:7:52 ratio (the same ratio used in $Pr_3Co_{2+x}Ge_7$)[1] inside an alumina crucible capped with an alumina frit and an inverted catch crucible,[18] then sealed inside a fused silica tube under ~1/3 atm of Ar gas. The sealed tube was heated in a programmable furnace to 1175 °C at 100°/h and dwelled for 24 h. The furnace was cooled slowly to 815 °C at 3°/h, at which point the tube was quickly removed, inverted, and centrifuged to remove excess flux. The tube was cracked open, and the hexagonal rod-shaped crystals of ~5 mm in length that were obtained are shown in Figure 1. The crystals were first etched with dilute HCl followed by water and acetone to remove any residual flux.

Table 3. Selected Interatomic Distances for $Yb_{0.5}Co_3Ge_3$ from Single Crystal X-ray Diffraction

sites	distance (Å)
Yb1–Ge1 (x6)	2.9415(6)
Yb1–Ge2 (x2)	2.6907(15)
Yb1–Ge3 (x2)	1.9568(5)
Co1–Co1 (x4)	2.5475(5)
Co1–Ge1 (x4)	2.4479(4)
Co1–Ge2 (x2)	2.6510(6)
Co1–Ge3 (x2)	2.5475(5)
Ge2–Ge2	2.446(3)
Yb–Yb (x6)	5.0949(10)
Yb–Yb (x2)	3.9136(9)

Table 4. Rietveld Refinement Results for $Yb_{0.5}Co_3Ge_3$

formula	$Yb_{0.456}Co_3Ge_{3.016}$
space group	*P6/mmm*
a (Å)	5.093492(12)
c (Å)	3.906482(10)
V (Å^3)	87.770(1)

Table 5. Atomic Positions for $Yb_{0.5}Co_3Ge_3$ from Rietveld Refinement

	x	*y*	*z*	occ.
Yb1	0	0	0	0.4557(5)
Co1	1/2	0	1/2	1
Ge1	1/3	2/3	0	1
Ge2	0	0	0.3067(2)	0.4557(5)
Ge3	0	0	1/2	0.1042(12)

2.2. Structure Determination. The crystal structure of $Yb_{0.5}Co_3Ge_3$ was determined using single crystal X-ray diffraction. Data were collected on a Bruker D8 Quest Kappa single crystal X-ray diffractometer equipped with an IμS microfocus source (Mo Kα, λ = 0.71073 Å), a HELIOS optics monochromator, and a PHOTON II CPAD detector. The Bruker SAINT program was used to integrate the diffraction data, while the absorption correction was performed using the Bruker program SADABS 2016/2 (multiscan method).[19] Starting models of $Yb_{0.5}Co_3Ge_3$ were obtained using the intrinsic phasing method in SHELXT,[20] and atomic sites were anisotropically refined using SHELXL2018.[21] The crystal structure of $Yb_{0.5}Co_3Ge_3$, a slightly disordered variant of the hexagonal YCo_6Ge_6 structure type, has unit cell dimensions of *a* = 5.0949(10) Å, *c* = 3.9136(9) Å, and *V* = 87.98(4) Å^3. Table 1 provides the crystallographic data and refinement parameters, Table 2 presents the atomic positions, and Table 3 lists selected bond distances for $Yb_{0.5}Co_3Ge_3$.

For the crystal structure determination, we started with a similar model as previously described for YCo_6Ge_6 and $YbCo_6Ge_6$.[4,5,22] This preliminary model contained a nearly half-occupied rare earth atomic site, 1*a* with fractional coordinates (0, 0, 0); a fully occupied Co atomic site, 3*g* with fractional coordinates (1/2, 0, 1/2); a fully occupied Ge atomic site, 2*c* with fractional coordinates (1/3, 2/3, 0);

Table 2. Atomic Positions for $Yb_{0.5}Co_3Ge_3$ from Single Crystal X-ray Diffraction

atom	Wyckoff site	*x*	*y*	*z*	occ.	U_{eq}[a] (Å^2)
Yb1	1*a* (6/*mmm*)	0	0	0	0.4633(9)	0.01023(15)
Co1	3*g* (*mmm*)	$^1/_2$	0	$^1/_2$	1	0.01013(13)
Ge1	2*c* (−6*m*2)	$^1/_3$	$^2/_3$	0	1	0.00743(13)
Ge2	2*e* (6*mm*)	0	0	0.3125(4)	0.4632(9)	0.0097(2)
Ge3	1*b* (6/*mmm*)	0	0	$^1/_2$	0.0736(19)	0.0097(2)

[a] U_{eq} is defined as $^1/_3$ of the trace of the orthogonalized U_{ij} tensor.

https://dx.doi.org/10.1021/acs.cgd.0c00865
Cryst. Growth Des. 2020, 20, 6715–6721

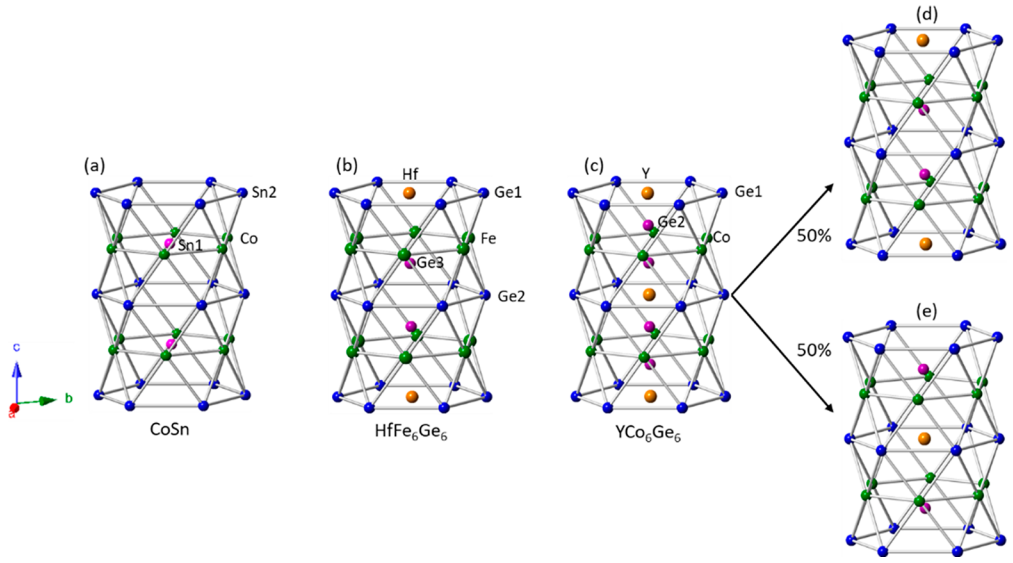

Figure 2. Crystal structures of (a) CoSn, (b) $HfFe_6Ge_6$, and (c) YCo_6Ge_6. The YCo_6Ge_6 structure exhibits structural disorder, and the two disordered structures, each occurring in 50% of cases, are displayed in (d) and (e). The orange spheres represent the rare-earth atoms that occupy the void spaces in the hexagonal channels. The pink and blue spheres represent the Sn and Ge atoms forming the structural framework with Fe/Co atoms (green spheres) residing within the framework. Some bonds have been omitted for the sake of clarity in these illustrations.

and a nearly half-occupied Ge atomic site, 2*e* with fractional coordinates (0, 0, *z*) where *z* = ~0.31. The nearly half-occupied rare earth site and nearly half-occupied Ge atomic site are due to the positional/occupational disorder that distinguishes the YCo_6Ge_6 structure type from the ordered $HfFe_6Ge_6$ structure type. The differences in these two structure types will be discussed in detail in the Results and Discussion section of this manuscript.

Residual electron density located at (0, 0, 1/2) is suggestive that there is slightly more disorder in $Yb_{0.5}Co_3Ge_3$ than in the YCo_6Ge_6 structure type. This density is also located in a similar location relative to the Co atoms as observed in the related CoSn structure type. Therefore, we expanded our preliminary model to represent a hybrid of the YCo_6Ge_6 structure type and CoSn structure type with the addition of a partially occupied Ge site (Ge3) with fractional coordinates (0, 0, 1/2). Since the Ge2 (6*mm*) and Ge3 (6/*mmm*) atoms can be thought of as having an occupancy dependent on that of Yb, the SUMP command was used. The Yb and Ge2 sites were fixed to refine to the same occupancy which is less than one. The Yb, Ge2, and Ge3 sites were constrained to unity. On the basis of our final model, it is suggestive that less than 8% of the unit cells adopt the related CoSn structure type, instead of the YCo_6Ge_6 structure type. Because of the structural similarities in the two structure types, this slight hybridization or slight defect does not seem unreasonable.

2.3. Powder X-ray Diffraction. Powder X-ray diffraction is an excellent complementary technique for distinguishing related phases and confirming the structural model as determined by single crystal X-ray diffraction. High resolution synchrotron powder X-ray diffraction data (λ = 0.412797 Å) were collected in the 2θ range from 0.5° to 50° at the 11-BM beamline at the Advanced Photon Source of Argonne National Laboratory. Discrete detectors collected data points every 0.001° 2θ with a scan speed of 0.01° s^{-1} at room temperature. Rietveld refinement, carried out with TOPAS-Academic software, was completed to confirm the disordered variant of the YCo_6Ge_6 structure type determined by single crystal X-ray diffraction. Table 4 gives the Rietveld refinement results for $Yb_{0.5}Co_3Ge_3$. Table 5 gives atomic positions for the structural model determined from Rietveld refinement, which agrees with the model determined from single crystal X-ray diffraction.

2.4. Properties Measurements. Temperature- and field-dependent magnetization measurements were performed on the Quantum Design MPMS 3 system. GE varnish was used to secure the sample and has a negligible contribution to the signal. Temperature-dependent resistivity was measured in a standard four-probe geometry (I = 1 mA) using the Quantum Design PPMS DynaCool. Electrical contacts to the samples were made with Au wires attached to the samples using EPOTEK silver epoxy and subsequently cured at 100 °C.

3. RESULTS AND DISCUSSION

3.1. Structure Determination. The CoSn structure type, shown in Figure 2a, crystallizes in the hexagonal *P6/mmm* space group with cell dimensions of *a* = 5.279(7) Å and *c* = 4.259(10) Å. This structure type is made up of two planar layers: the Co kagome nets centered by Sn atoms and a second

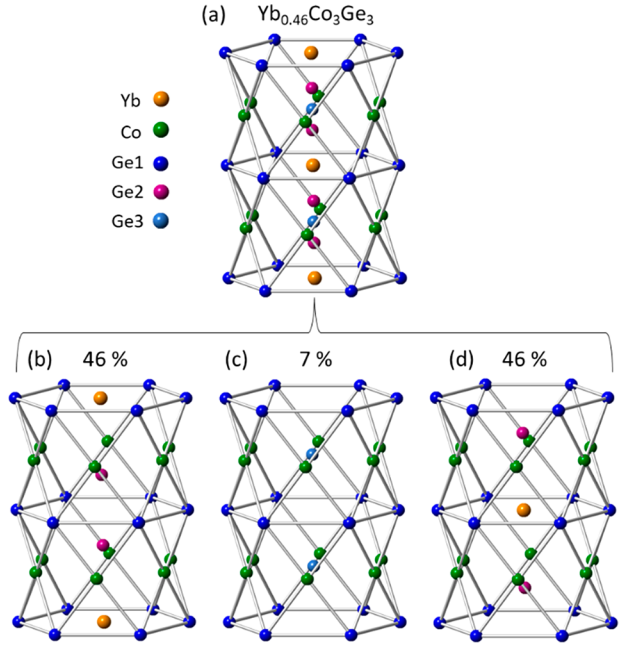

Figure 3. Crystal structure of $Yb_{0.5}Co_3Ge_3$ where (a) shows all possible atomic positions, (b) and (d) show YCo_6Ge_6 type arrangements each with 46% occupancy, and (c) shows CoSn type arrangement with 7% occupancy.

https://dx.doi.org/10.1021/acs.cgd.0c00865
Cryst. Growth Des. 2020, 20, 6715−6721

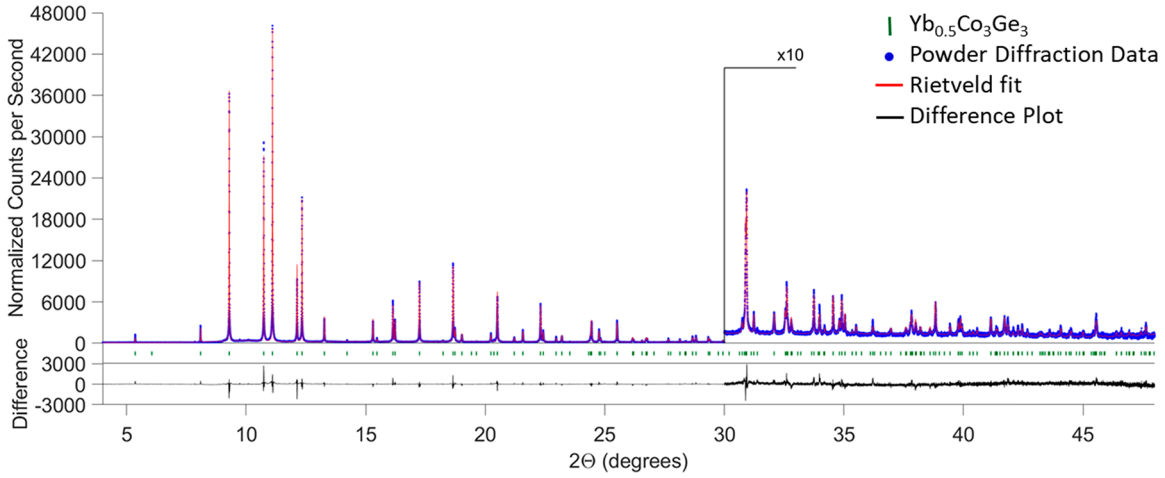

Figure 4. Observed (blue dots), calculated (red line), and difference (black line, bottom) synchrotron powder X-ray diffraction patterns for $Yb_{0.5}Co_3Ge_3$ by the Rietveld analysis technique. The difference pattern is plotted at the same scale as the other peaks.

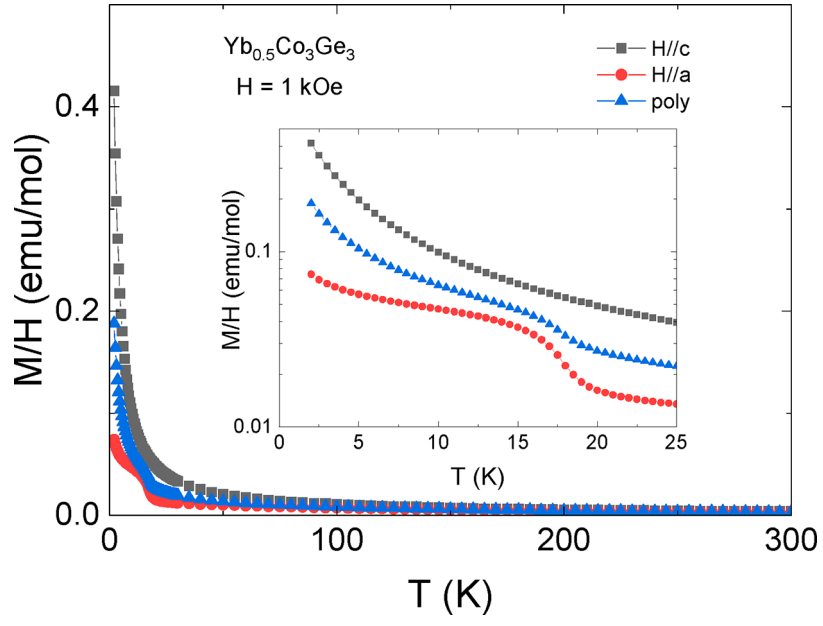

Figure 5. Temperature-dependent magnetization for $Yb_{0.5}Co_3Ge_3$ measured at 1 kOe.

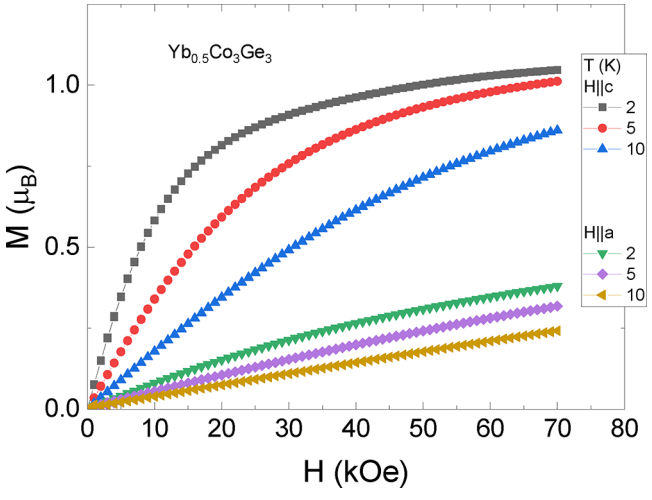

Figure 6. Field-dependent magnetization of $Yb_{0.5}Co_3Ge_3$ measured at 2, 5, and 10 K.

hexagonal Sn segment stacked alternately in the *c* direction.[23] The Co and Sn atoms form a close-packed layer with each Sn1 atoms surrounded by six Co atoms (Co−Sn(1) distance of 2.6395(3) Å). In the next layer, the Sn atoms are located in Co trigonal prisms with a bond distance of 2.6190(4) Å, resulting in hexagonal channels centered by the first Sn atoms. The Sn layer contains half the number of atoms compared to the close-packed layer resulting in condensed trigonal bipyramids.[11,12] Depending on the relative positions of guest atoms and capping of the M atoms corresponding to the MT_6X_6 in the CoSn host structure, these intermetallics can adopt hexagonal $HfFe_6Ge_6$-type (H-type) or hexagonal YCo_6Ge_6-type (Y-type, a disordered variant of H-type).[24−27] The H-type $HfFe_6Ge_6$, *P6/mmm* space group with cell dimensions of a = 5.065 Å and c = 8.058 Å,[24,27−29] is formed by "stuffing" Hf atoms into the hexagonal voids of the FeGe (CoSn-type) framework. Figure 2b shows the stacked layers of alternate filled and empty planes of the $HfFe_6Ge_6$ (H-type) crystal structure. Such ordering of Hf atoms in the alternate layers results in doubling of the unit cell along the c direction.[25,26] The Y-type, YCo_6Ge_6 structure

https://dx.doi.org/10.1021/acs.cgd.0c00865
Cryst. Growth Des. 2020, 20, 6715−6721

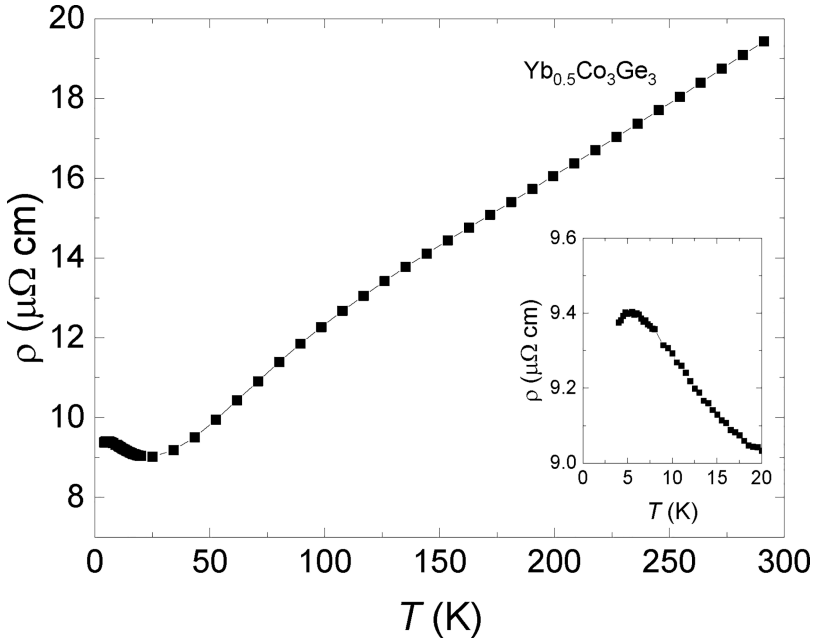

Figure 7. Temperature-dependent resistivity of $Yb_{0.5}Co_3Ge_3$ with inset showing enlarged view below T = 20 K..

(also represented as $Y_{0.5}Co_3Ge_3$),[22] also crystallizes in the *P6/mmm* space group with unit cell dimensions of a = 5.074 Å, c = 3.908 Å.[22−30] Figure 2c shows the YCo_6Ge_6 structure type, formed by stuffing Y atoms into a CoGe (CoSn-type) hexagonal framework. In contrast to the order of the Hf atoms in the H-type, the Y atoms in this structure type are occupationally disordered.[24,26] Despite the similarity of the H-type $HfFe_6Ge_6$ and Y-type YCo_6Ge_6 structures, they are distinguishable by powder diffraction by the d spacing of the (001) reflection.

Figure 3 shows the crystal structure of title compound $Yb_{0.5}Co_3Ge_3$, a slight hybridization of the YCo_6Ge_6 structure type with the CoSn structure type, crystallizing in the *P6/mmm* space group with lattice parameters $a \approx 5.1$ Å and $c \approx 3.9$ Å as determined from both single crystal and synchrotron powder X-ray diffraction. The $Yb_{0.5}Co_3Ge_3$ crystal structure consists of one Yb site, one Co site, and three Ge sites. The Ge2 (*6mm*) and Ge3 (*6/mmm*) atoms can be thought of having an occupancy dependent on that of Yb. As shown in Figure 3b,d, the $Yb_{0.5}Co_3Ge_3$ compound displays structural disorder similar to YCo_6Ge_6 (Figure 2d,e). However, in the Yb analogue, a third possibility exists, shown in Figure 3c, when the Yb atom is not present along the *c*-axis, the Ge3 atom occupies the *6/mmm* position in a CoSn-type arrangement with a 7% occupancy. The refined unit cell parameters from powder X-ray diffraction of $Yb_{0.5}Co_3Ge_3$ are a = 5.093492(12) Å, c = 3.906482(10) Å, V = 87.770(1) Å^3 which are in reasonable agreement with the single crystal data of $Yb_{0.5}Co_3Ge_3$ as well as the original report of the $YbCo_6Ge_6$ crystal structure (of the ordered YCo_6Ge_6 type).[5] Refinement of the rare earth site reveals that the Yb occupancy is 0.4557(5), which agrees with the occupancy as determined by single crystal X-ray diffraction, 0.4633(9). The disordered Ge sites refine to occupancies of 0.4557(5) and 0.1042(12), agreeing with the single crystal X-ray diffraction values of 0.4632(9) and 0.0736(19) for Ge2 and Ge3, respectively. In Figure 4, the observed powder diffraction data (blue dots), calculated Rietveld fit (red line), and difference plot (black line, bottom) are illustrated. The row of green tick marks indicates the calculated peak positions. The difference pattern is plotted at the same scale as the other patterns. Above 30° 2θ (synchrotron wavelength of 0.412797 Å), the intensity scale of all patterns has been magnified 10 times.

3.2. Physical Properties. $Yb_{0.5}Co_3Ge_3$ (originally denoted as $YbCo_6Ge_6$) was first reported to adopt the YCo_6Ge_6 structure type.[4,5] The polycrystalline phase as obtained by arc-melting was characterized by powder X-ray diffraction, and magnetic susceptibility measurements collected from 78 to 293 K indicate that the phase is paramagnetic. The effective moment obtained from the Curie−Weiss fit is μ_{eff} = 4.56 μ_B, close to the calculated Yb^{3+} moment (μ_{eff} = 4.54 μ_B), and the Weiss constant of −31 K indicates antiferromagnetic interactions are dominant.[5]

The temperature-dependent magnetization for single crystals of $Yb_{0.5}Co_3Ge_3$ grown for this work was measured from 2 to 300 K as shown in Figure 5. The magnetic susceptibility data were fit from 150 to 300 K. The effective magnetic moment as obtained from the Curie−Weiss fit is 4.23 μ_B, which is slightly less than what is expected for Yb^{3+} (μ_{eff} = 4.54 μ_B). Weiss constants for H//*a*, H//*c*, and the polycrystalline average are −21 K, −18.7 K, and −21 K, respectively. The antiferromagnetic dominant interactions, as indicated by the negative Weiss constants, along with the absence of magnetic ordering suggests geometric frustration. A feature between 15 and 20 K, only visible in the H//*a* and polycrystalline data, suggests spin canting or spin reorientation. Figure 6 shows the field-dependent magnetization at 2, 5, and 10 K. The magnetization is larger for H//*c*, indicating it as the easy axis, which is reasonable given the Yb−Yb distance of 3.9136(9) Å in the *c* direction and 5.0949(10) Å in the *a* direction. At 2 K, magnetization begins to saturate ∼1 μ_B, lower than the full saturation magnetic moment of Yb^{3+} (4.00 μ_B), which can be attributed to crystal electric field effects or possible valence fluctuation. Figure 7 shows electrical resistivity as a function of temperature. The high temperature peak at ∼100 K is most likely a consequence of the depopulation of the CEF levels as

https://dx.doi.org/10.1021/acs.cgd.0c00865
Cryst. Growth Des. 2020, 20, 6715−6721

the temperature is lowered. The low temperature peak at ∼5.5 K could either be due to the low lying CEF levels or a magnetic phase transition. Heat capacity and/or neutron diffraction measurements are necessary to elucidate the origin of this maximum. Given the possibility of Yb undergoing valence fluctuation, future experiments are ongoing to correlate the transport properties with the change in oxidation state.

4. CONCLUSION

In this manuscript, we present the crystal growth and structure determination of $Yb_{0.5}Co_3Ge_3$ and compare this with the $HfFe_6Ge_6$ and YCo_6Ge_6 structure types. Both H-type and Y-type structures can be considered "stuffed" variants of the CoSn structure. Our metal-flux synthesis of $Yb_{0.5}Co_3Ge_3$ resulted in a hybrid Y-type/7CoSn-type structure. We refined the structural model using single crystal and synchrotron powder X-ray diffraction data and determined that $Yb_{0.5}Co_3Ge_3$ contains ∼7% CoSn-type. The results of this work demonstrate the ability of guest atoms to substantially alter stability, which may be useful in the future design of magnetic materials.[31,32] The complementary use of single crystal and powder X-ray diffraction is a powerful way to model new structures and distinguish between similar structure types. Rietveld refinement of synchrotron powder X-ray diffraction data was particularly helpful in confirming the structural disorder of $Yb_{0.5}Co_3Ge_3$. Especially in the field of intermetallics, the complementary use of Rietveld methods is critical to confirming the structural details of complex materials.

■ ASSOCIATED CONTENT

Accession Codes

CCDC 2010706 (for $Yb_{0.5}Co_3Ge_3$) contains the supplementary crystallographic data for this paper. These data can be obtained free of charge via www.ccdc.cam.ac.uk/data_request/cif, or by emailing data_request@ccdc.cam.ac.uk, or by contacting The Cambridge Crystallographic Data Centre, 12 Union Road, Cambridge CB2 1EZ, UK; fax: +44 1223 336033.

■ AUTHOR INFORMATION

Corresponding Author

Julia Y Chan − *Department of Chemistry and Biochemistry, University of Texas at Dallas, Richardson, Texas 75080, United States;* orcid.org/0000-0003-4434-2160; Email: Julia.Chan@utdallas.edu

Authors

Ashley Weiland − *Department of Chemistry and Biochemistry, University of Texas at Dallas, Richardson, Texas 75080, United States;* orcid.org/0000-0001-7198-3559

Lucas J. Eddy − *Department of Chemistry and Biochemistry, University of Texas at Dallas, Richardson, Texas 75080, United States*

Gregory T. McCandless − *Department of Chemistry and Biochemistry, University of Texas at Dallas, Richardson, Texas 75080, United States*

Halyna Hodovanets − *Maryland Quantum Materials Center, Department of Physics, University of Maryland, College Park, Maryland 20742, United States*

Johnpierre Paglione − *Maryland Quantum Materials Center, Department of Physics, University of Maryland, College Park, Maryland 20742, United States; Canadian Institute for Advanced Research, Toronto, Ontario M5G 1Z8, Canada*

Complete contact information is available at: https://pubs.acs.org/10.1021/acs.cgd.0c00865

Notes

The authors declare no competing financial interest.

■ ACKNOWLEDGMENTS

This material is based upon work supported by the U.S. Department of Energy, Office of Science, Office of Workforce Development for Teachers and Scientists, Office of Science Graduate Student Research (SCGSR) program. The SCGSR program is administered by the Oak Ridge Institute for Science and Education for the DOE under Contract No. DE-SC0014664. J.Y.C. acknowledges National Science Foundation Grant No. DMR-1700030 for support of this project. Experimental investigations at the University of Maryland were supported by the Gordon and Betty Moore Foundation's EPiQS Initiative through Grant No. GBMF9071. A.W. acknowledges the support of the Eugene McDermott Graduate Fellows Program. The authors thank Justin B. Felder for assistance with synthesis and Saul Lapidus for useful discussion and guidance. The authors declare no competing interests.

■ REFERENCES

(1) Khan, M. A.; McCandless, G. T.; Benavides, K. A.; Martin, T. J.; Palacios, A. M.; Samuel, A. W. B.; Young, D. P.; Chan, J. Y. Crystal Growth and Magnetic Properties of $Pr_3Co_{2+x}Ge_7$ and the Sn-Stabilized $Ln_3Co_{2+x}Ge_{7-y}Sn_y$ (Ln = Pr, Nd, Sm). *Cryst. Growth Des.* **2018**, *18*, 6028−6034.

(2) Felder, J. B.; Weiland, A.; Hodovanets, H.; McCandless, G. T.; Estrada, T. G.; Martin, T. J.; Walker, A. V.; Paglione, J.; Chan, J. Y. Law and Disorder: Special Stacking Units-Building the Intergrowth $Ce_6Co_5Ge_{16}$. *Inorg. Chem.* **2019**, *58*, 6037−6043.

(3) Weiland, A.; Felder, J. B.; McCandless, G. T.; Chan, J. Y. One Ce, Two Ce, Three Ce, Four? An Intermetallic Homologous Series to Explore: $A_{n+1}B_nX_{3n+1}$. *Chem. Mater.* **2020**, *32*, 1575−1580.

(4) Dzyanyi, R. B.; Bodak, O. I.; Aksel'Rud, L. G.; Pavlyuk, V. V. Crystal Structure of YbM_6Ge_6 (M: Fe, Co, Mn) Compounds. *Inorg. Mater.* **1995**, *31*, 910.

(5) Fedyna, M.; Skolozdra, R.; Gorelenko, Y. K. Magnetic and Electric Properties of RCo_6Ge_6 (R-Y, Dy, Er-Lu). *Neorg. Mater.* **1999**, *35*, 461−463.

(6) Kida, T.; Fenner, L. A.; Dee, A. A.; Terasaki, I.; Hagiwara, M.; Wills, A. S. The Giant Anomalous Hall Effect in the Ferromagnet Fe_3Sn_2—a Frustrated Kagome Metal. *J. Phys.: Condens. Matter* **2011**, *23*, 112205.

(7) Yazyev, O. V. An Upside-Down Magnet. *Nat. Phys.* **2019**, *15*, 424−425.

(8) Wang, Q.; Xu, Y.; Lou, R.; Liu, Z.; Li, M.; Huang, Y.; Shen, D.; Weng, H.; Wang, S.; Lei, H. Large Intrinsic Anomalous Hall Effect in Half-Metallic Ferromagnet $Co_3Sn_2S_2$ with Magnetic Weyl Fermions. *Nat. Commun.* **2018**, *9*, 3681.

(9) Liu, E.; Sun, Y.; Kumar, N.; Muechler, L.; Sun, A.; Jiao, L.; Yang, S.-Y.; Liu, D.; Liang, A.; Xu, Q.; Kroder, J.; Süß, V.; Borrmann, H.; Shekhar, C.; Wang, Z.; Xi, C.; Wang, W.; Schnelle, W.; Wirth, S.; Chen, Y.; Goennenwein, S. T. B.; Felser, C. Giant Anomalous Hall Effect in a Ferromagnetic Kagome-Lattice Semimetal. *Nat. Phys.* **2018**, *14*, 1125−1131.

(10) Yang, T. Y.; Wan, Q.; Wang, Y. H.; Song, M.; Tang, J.; Wang, Z. W.; Lv, H. Z.; Plumb, N. C.; Radovic, M.; Wang, G. W.; Wang, G. Y.; Sun, Z.; Yu, R.; Shi, M.; Xiong, Y. M.; Xu, N., Evidence of Orbit-Selective Electronic Kagome Lattice with Planar Flat-Band in Correlated Paramagnetic YCr_6Ge_6. *arXiv e-prints* **2019**, arXiv:1906.07140.

(11) Larsson, A. K.; Haeberlein, M.; Lidin, S.; Schwarz, U. Single Crystal Structure Refinement and High-Pressure Properties of CoSn. *J. Alloys Compd.* **1996**, *240*, 79−84.
(12) Simak, S. I.; Häußermann, U.; Abrikosov, I. A.; Eriksson, O.; Wills, J. M.; Lidin, S.; Johansson, B. Stability of the Anomalous Large-Void CoSn Structure. *Phys. Rev. Lett.* **1997**, *79*, 1333−1336.
(13) Parthé, E. Space Filling of Crystal Structures. *Z. Kristallogr.* **1961**, *115*, 52.
(14) Kang, M.; Ye, L.; Fang, S.; You, J.-S.; Levitan, A.; Han, M.; Facio, J. I.; Jozwiak, C.; Bostwick, A.; Rotenberg, E.; Chan, M. K.; McDonald, R. D.; Graf, D.; Kaznatcheev, K.; Vescovo, E.; Bell, D. C.; Kaxiras, E.; van den Brink, J.; Richter, M.; Prasad Ghimire, M.; Checkelsky, J. G.; Comin, R. Dirac Fermions and Flat Bands in the Ideal Kagome Metal FeSn. *Nat. Mater.* **2020**, *19*, 163−169.
(15) Canfield, P. C.; Fisk, Z. Growth of Single Crystals from Metallic Fluxes. *Philos. Mag. B* **1992**, *65*, 1117−1123.
(16) Canfield, P. C.; Fisher, I. R. High-Temperature Solution Growth of Intermetallic Single Crystals and Quasicrystals. *J. Cryst. Growth* **2001**, *225*, 155−161.
(17) Phelan, W. A.; Menard, M. C.; Kangas, M. J.; McCandless, G. T.; Drake, B. L.; Chan, J. Y. Adventures in Crystal Growth: Synthesis and Characterization of Single Crystals of Complex Intermetallic Compounds. *Chem. Mater.* **2012**, *24*, 409−420.
(18) Canfield, P. C.; Kong, T.; Kaluarachchi, U. S.; Jo, N. H. Use of Frit-Disc Crucibles for Routine and Exploratory Solution Growth of Single Crystalline Samples. *Philos. Mag.* **2016**, *96*, 84−92.
(19) Krause, L.; Herbst-Irmer, R.; Sheldrick, G.; Stalke, D., Comparison of Silver and Molybdenum Microfocus X-ray Sources for Single-Crystal Structure Determination. *J. Appl. Crystallogr.* **2015**, *48*.
(20) Sheldrick, G. M. SHELXT - Integrated Space-Group and Crystal-Structure Determination. *Acta Crystallogr., Sect. A: Found. Adv.* **2015**, *71*, 3−8.
(21) Sheldrick, G. M. Crystal Structure Refinement with SHELXL. *Acta Crystallogr., Sect. C: Struct. Chem.* **2015**, *71*, 3−8.
(22) Buchholz, W.; Schuster, H. U. Intermetallic Phases with B35-Superstructure and Relationship to $LiFe_6Ge_6$. *Z. Anorg. Allg. Chem.* **1981**, *482*, 40−48.
(23) Nial, O. X-Ray Examination of Cobalt-Tin alloys and a Comparison of the System Co - Sn with Fe - Sn and Ni - Sn. *Z. Anorg. Allg. Chem.* **1938**, *238*, 287−296.
(24) Szytula, A.; Leciejewicz, J. *Handbook of Crystal Structures and Magnetic Properties of Rare Earth Intermetallics*, 1st ed.; CRC: Boca Raton, 1994.
(25) Venturini, G. Filling the CoSn Host-Cell: The $HfFe_6Ge_6$-Type and the Related Structures. *Z. Kristallogr. - Cryst. Mater.* **2006**, *221*, 511. DOI: 10.1524/zkri.2006.221.5-7.511
(26) Venturini, G. G.; Lefèvre, H. I.-m. C.; Lidin, S.; Malaman, B.; Mazet, T.; Tobola; Vernière, A.; Ihou-Mouko, H. Structures and Crystal Chemistry of MT_6X_6 Phases, Filled Derivatives of the CoSn-B35 Structure. *Chem. Met. Alloys* **2008**, *1*, 24−33.
(27) Salamakha, P. S. *Crystal Structures and Crystal Chemistry of Ternary Rare-Earth Germanides*; Elsevier, 1999; Vol. *27*, p 225−338.
(28) Olenich, R. R.; Aksel'rud, L. G.; Yarmolyuk, Y. R. Crystal Structure of Ternary Germanides RFe_6Ge_6 (R = Sc, Ti, Zr, Hf, Nd) and RCo_6Ge_6 (R= Ti, Zr, Hf). *Dopov. Akad. Nauk Ukr.* **1981**, 84−88.
(29) Venturini, G.; Welter, R.; Malaman, B. Crystallographic Data and Magnetic Properties of RT_6Ge_6 Compounds (R = Sc, Y, Nd, Sm, Gd-Lu; T = Mn, Fe). *J. Alloys Compd.* **1992**, *185*, 99−107.
(30) Mruz, O. Y.; Starodub, P. K.; Bodak, O. I. New Representatives of the YCo_6Ge_6 Structure Type. *Dopov. Akad. Nauk Ukr. RSR, Ser. B* **1984**, 45−47.
(31) Fulfer, B. W.; McAlpin, J. D.; Engelkemier, J.; McCandless, G. T.; Prestigiacomo, J.; Stadler, S.; Fredrickson, D. C.; Chan, J. Y. Filling in the Holes: Structural and Magnetic Properties of the Chemical Pressure Stabilized $LnMn_xGa_3$ (Ln = Ho−Tm; $x < 0.15$). *Chem. Mater.* **2014**, *26*, 1170−1179.
(32) Benavides, K. A.; Treadwell, L. J.; Campbell, G. D.; McDougald, R. N.; McCandless, G. T.; Chan, J. Y. Structural Stability and Magnetic Properties of LnM_xGa_3 (Ln = Ho, Er; M = Fe, Co; $x < 0.2$). *Polyhedron* **2016**, *114*, 56−61.

https://dx.doi.org/10.1021/acs.cgd.0c00865
Cryst. Growth Des. 2020, 20, 6715−6721